HardwareX 10 (2021) e00246

Contents lists available at ScienceDirect

HardwareX

journal homepage: www.elsevier.com/locate/ohx

Automated melt electrowritting platform with real-time process monitoring

Pawel Mieszczanek [a,b,*], Sebastian Eggert [c], Peter Corke [d,e], Dietmar W. Hutmacher [a,b,f,*]

[a] Centre in Transformative Biomimetics in Bioengineering, Queensland University of Technology, Brisbane, QLD 4000, Australia
[b] School of Mechanical, Medical and Process Engineering, Faculty of Engineering, Queensland University of Technology, Brisbane, QLD 4000, Australia
[c] Department of Mechanical Engineering, Technical University of Munich, Garching 85748, Germany
[d] QUT Centre for Robotics, Queensland University of Technology, Brisbane, QLD 4000, Australia
[e] School of Electrical Engineering and Robotics, Faculty of Engineering, Queensland University of Technology, Brisbane, QLD 4000, Australia
[f] ARC ITTC in Additive Biomanufacturing, Queensland University of Technology, Brisbane, QLD 4000, Australia

ARTICLE INFO

Article history:
Received 12 August 2021
Received in revised form 29 October 2021
Accepted 4 November 2021

Keywords:
3D printing
Melt electrowriting
Automation
Process monitoring
Additive manufacturing

ABSTRACT

Melt electrowriting (MEW) is an additive manufacturing (AM) technology with the ability to fabricate complex designs with high-resolution. The utility of MEW is studied in many fields including tissue engineering and soft robotics. However, current MEW hardware offers only basic functionality and is often designed and built in-house. This affects results replication across different MEW devices and slows down the technological advancement. To address these issues, we present an automated MEW platform with real-time process parameter monitoring and control. We validate the developed platform by demonstrating the ability to accurately print polymer structures and successfully measure and adjust parameters during the printing process. The platform enables the collection of large volumes of data that can be subsequently used for further analysis of the system. Ultimately, the concept will help MEW to become more accessible for both research laboratories and industry and allow advancing the technology by leveraging the process monitoring, control and data collection.

Table Specifications table

Hardware name	*Automated Melt Electrowritting Platform with Real-time Process Monitoring*
Subject area	*Please select the subject area most relevant to the original community for which this hardware was developed* • Engineering and Material Science • Chemistry and Biochemistry

(*continued on next page*)

* Corresponding authors at: Centre in Transformative Biomimetics in Bioengineering, Queensland University of Technology, Brisbane, QLD 4000, Australia.
E-mail addresses: pawel.mieszczanek@qut.edu.au (P. Mieszczanek), dietmar.hutmacher@qut.edu.au (D.W. Hutmacher).

https://doi.org/10.1016/j.ohx.2021.e00246
2468-0672/

Hardware type	• Medical (e.g. Pharmaceutical Science) • Biological Sciences (e.g. Microbiology and Biochemistry) • Educational Tools and Open-source Alternatives to Existing Infrastructure • Imaging tools • Measuring physical properties and in-lab sensors • Electrical engineering and computer science • Mechanical engineering and materials science
Open-source License	*Creative Commons Attribution-ShareAlike 4.0 International (CC BY-SA 4.0)*
Cost of Hardware	*Mechanical hardware: $1950Electrical hardware: $8100*
Source File Repository	https://doi.org/10.5281/zenodo.4699811 https://github.com/Lasonic/automated_mew_platform

1. Hardware in context

Additive manufacturing (AM), commonly referred to as 3D printing, describes a process where the material is deposited in a layer-by-layer fashion to manufacture precise geometric shapes. Initially, AM was used mostly as a rapid prototyping tool due to the low manufacturing costs and fast turnaround of small batch sizes. However, recent hardware and software development enabled the technology to be applied in different industries such as the medical [1–5] and aerospace sectors [6–9], as a valuable method to manufacture the final product. Particularly for medical applications, AM is increasingly used to manufacture personalised implants [10], prosthetics [11], and anatomical models [12]. While common AM techniques, such as Fused Deposition Modelling or Selective Laser Sintering are now well-established manufacturing platforms, they are limited in terms of printing resolution. High-resolution is, in particular, essential for the production of highly porous meshes or scaffolds used in tissue engineering, regenerative medicine and soft robotics [13–17].

For this reason, a relatively young yet quickly emerging AM technique known as melt electrowriting (MEW) attracted attention due to the capability of fabricating well-organised and microscaled fibre structures using biocompatible and biodegradable polymers [18–20]. The main principle and signature of MEW is a strong electric field established between the nozzle and collector plate which enables the fabrication of fibres in the range of 0.8–50 μm [21].

To date, commercially available MEW hardware is attached to expensive bioprinters, yet only offer low throughput printing of very simple geometries. Hence, only a small fraction of the current MEW literature cites these commercial devices. Most of the currently used MEW printers were designed and manufactured in academic lab settings which are usually not equipped for developing industrial level and well-engineered printers. Although MEW applications have been frequently reported in recent years [21], they lack the description of the specific hardware components, build instructions, and software control. This has resulted in a spectrum of MEW machines, each producing the data that is not comparable with each other. Since the replication of results across different MEW devices is not possible, the users have to spend a substantial amount of time on the adjustment of the process parameters. As a result, one of the main bottlenecks in MEW is the lack of reproducibility of the printed structures caused mainly by the incorrectly selected input parameters across many custom-built MEW printers. This results in unstable printing conditions that affect the reproducibility and quality of the fabricated porous structures [22,23].

In order to study and develop a deeper understanding of the effect of different combinations of input parameters on the quality of the printed fibres, a monitoring system is used to obtain a live video stream of the fibre deposition process. Recent studies confirmed that real-time monitoring and process control significantly increase automation of the process and reveal underlying information about the correlation between parameters in MEW [24,25]. Furthermore, by analysing the jet pattern, the stability, and therefore reproducibility, of the process can be improved [27,23]. Although process monitoring has been proven as an essential addition to MEW, the vast majority of the currently utilised MEW hardware does not offer real-time monitoring and control functionality.

Here, we aim to address these limitations by developing an automated MEW device with real-time monitoring and parameter control capabilities. The main objective of the MEW platform was to achieve (i) automated digital printing parameter control with (ii) real-time process monitoring functionality with (iii) the cost-effective, yet robust and (iv) flexible design for further platform development according to the user-specific needs. Finally, (v) an open-source format of this submission will help MEW to become more accessible within the research community and will ultimately lead to the commercialization of printers demonstrating a cutting-edge performance.

2. Hardware description

The automated MEW setup was divided into electrical, mechanical, firmware and software design. Each section describes the solution to achieve the aforementioned objectives and provides a detailed overview of the hardware used in the MEW platform. A summary of the advantages and limitation of the hardware is shown in Table 1.

Table 1
Summary of advantages and limitations of the MEW automated platform.

Advantages	• Printing automation • Digitally controlled MEW device • Real-time input parameter control • Real-time output parameter monitoring • A foundation for further research and development • Simple to implement design • Ideal for prototyping • Inexpensive yet accurate and robust solution
Limitations	• Large size for a 3D printer • Weight • Requires a wide range of basic skills from multiple engineering disciplines (mechanical, electrical and software engineering)

2.1. Electrical design

An overview of the electrical design is shown in Fig. 1. The core of the system is two microcontroller-based boards that are responsible for temperature, pressure, high voltage and motion control. Sensors, actuators and controller boards were selected, followed by an establishment of an inter-system communication protocol between the control and computing unit to allow for data transfer.

Embedded control unit

The control unit consists of Smoothieboard (The Smoothie project, http://smoothieware.org) and Arduino Due (Arduino, Italy). Smoothieboard is an open-source microcontroller board based on ARM Cortex-M3 microcontroller unit designed to run 3D printers, lasers, CNC mills/routers – devices that are based on a multi-axis linear system. It has well-written documentation and instructions available online (see Supporting Table T1). In the MEW platform, Smoothieboard is used to control a system of three linear actuators, a printhead heating system as well as communicate with the computing unit via serial over USB connection. Additionally, the open-source firmware can be easily modified via a configuration file, which makes it a suitable solution for beginners as well as advanced users. Arduino Due is a microcontroller board based on the ARM Cortex-M3 microcontroller unit. Similarly, Arduino is an open-source platform with a community-driven forum and extensive documentation of each device (see Supporting Table T1). In the MEW platform, Arduino Due is used to control inputs such as high voltage and air pressure.

Computing unit

The previously mentioned computing unit is a PC (Windows 10, Inter Core i7,16 GB RAM) which serves as a link between two microcontroller boards. The computing unit is used to send and receive commands with the Smoothieboard and Arduino Due using Python user interface over USB ports. This allows for real-time control and monitoring of the printing process.

Motion control

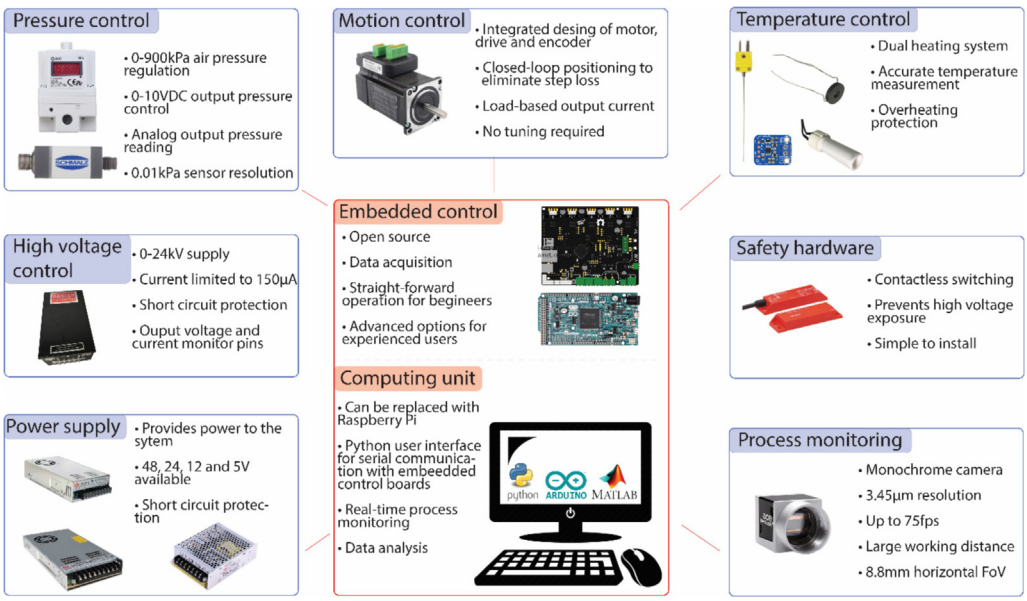

Fig. 1. Electrical design overview of an Automated MEW platform consists of power supply units, high voltage control, pressure control, motion control, temperature control, safety hardware and process monitoring devices.

The motion control system consists of three closed-loop stepper servo motors (StepperOnline, China) that run a 3-axis linear actuator setup. The optical encoder allows for a closed-loop operation to eliminate positioning error. The motors have integrated drives that are controlled via Smoothieboard.

Process monitoring

Process monitoring is performed using a digital camera (Edmund Optics, USA) and lens (Edmund Optics, USA) setup. The combination provides high-resolution imaging (camera pixel size of 3.45 $\times$ 3.45 μm) that is used to record the process of fibre deposition. This, in turn, allows for a very detailed analysis of the process output.

Temperature control

The temperature of the filament is controlled using a dual heating system of the printhead. The lower ring-shaped heater (Rauschert, Germany) is targeted at a nozzle while the upper heater (Rauschert, Germany) controls the temperature of the polymer stored in a syringe. The temperature set by both heaters is measured via two k-type thermocouples (RS Components, Australia). The Smoothieboard controls the heating system to maintain the desired temperature of both heaters.

High voltage

The high voltage (HV) of the system is delivered via an HV unit (Gamma High Voltage Research, USA). The output of the HV unit is easily controlled with analog input voltage. Additionally, it has analog output monitors which allow for output voltage and current monitoring. The Arduino Due controls the HV output as well as monitoring the output voltage and current.

Pneumatic pressure system

The pressure system is based on a pneumatic pressure regulator (SMC, USA). Input to the regulator is supplied by an external source of pressurised air, while the output pressure is controlled by an analog voltage and monitored by a pressure sensor (Schmalz, Germany) that outputs an analog voltage. Both pressure regulator and sensor are controlled via Arduino Due.

Power unit

The power system consists of three power supply units (PSU). First, 48VDC 320 W PSU (MeanWell, USA) supplies power to the stepper motors. Second, 12VDC 240 W PSU (MeanWell, USA) provides power to Smootieboard and heating elements. Lastly, a dual output 24/5 VDC 120 W PSU (MeanWell, USA) supplies power to the pressure regulator, pressure sensor and HV unit.

Safety hardware

Working with HV raises potential safety hazards. To minimise them, a pair of non-contact magnetic switches (Telemecanique sensors, France) was coupled with the front door of the device in order to shut the power supply to the HV unit when a user attempts to access the inside of the printer during operation.

2.2. Firmware and software design

A Python user interface was developed to run on the computing unit to control both microcontroller boards. Together with the firmware designed for both the Arduino and Smoothieboard, they allow to capture the data from the sensors as well as adjust the input parameters during the printing process.

Embedded firmware

Firmware was developed and configured for both the Arduino and Smoothieboard microcontrollers, respectively. Arduino firmware can be uploaded via any platform that supports Arduino IDE. In this case, the previously described computing unit was used to develop and upload the program onto the Arduino. Custom Arduino firmware was written to collect data from the sensors and send the commands to the actuators when requested. Communication between a user (or another program) and the Arduino is done via USB port or UART serial communication port. While the serial communication can be easily established over the USB port by simply connecting the microcontroller to the computing unit, the USB to TTL UART adapter must be used to connect both devices over the UART port. The smoothieboard runs an open-source firmware called Smoothie – a high-performance G-code interpreter. The firmware can be configured via an editable configuration file stored on the Smoothieboard's SD card. Similarly, the Smoothieboard uses serial communication to exchange information with other devices over the USB or UART port. Since Smoothie is primarily a G-code interpreter, it supports a wide range of G-codes that are used for communication with the board. Furthermore, it also offers SimpleShell – a Unix-like module that provides an additional set of available commands.

Communication protocol

A custom serial communication protocol that provides a framework to allow sending and receiving packets was established as a part of the developed firmware. The UART port on each microcontroller is used to send and receive data from the computing unit via the USB to TTL UART adapter (Core electronics, Australia). The asynchronous serial interface at the baud rate of 115,200 is used to allow the communication with the Arduino. Unlike Arduino, Smoothie includes a communication protocol defined by the G-code interpreter and SimpleShell. Similarly, the asynchronous serial interface at the baud rate of 115,200 is used.

Python user interface

A Python user interface was developed to allow a user to communicate with both Smoothieboard and Arduino Due. The program starts serial communication with both microcontroller boards via serial ports specified by the user. The interface allows to send commands and, if applicable, receive the data from one board at a time.

2.3. Mechanical design

An overview of the mechanical design is shown in Fig. 2. The framework is based on aluminium extrusions and provides mechanical support for the linear stages which in turn support both the print bed and printhead. The print bed movement is performed in x and y-direction via a pair of linear actuators, while the printhead is supported by a third linear actuator that allows for position adjustment along the z-axis.

Framework

A mechanical frame that provides structural support is based on aluminium profiles. The profiles are easy to access and can be mounted together using corner brackets. Therefore, the assembly is quick, simple and provides flexibility to customise the design if necessary. The framework was designed to separate most of the electrical devices from the printing space. Electrical hardware was fixed onto a withdrawable aluminium plate in the bottom section of the framework while the top section was dedicated only for sensors and actuators that are used to directly control or monitor the printing process.

Enclosure

The platform's enclosure is made of acrylic panels. Matt black acrylic was chosen in order to minimise the light reflection that might affect the accuracy of the monitoring system. The enclosure was designed in a way that allows acrylic panels to be assembled independently from any other subsystem of the platform. Therefore, an acrylic enclosure can be installed once the other components are in place.

Printhead

The body of the printhead is made of the cylindrical-shaped teflon part that ensures good thermal properties. It was designed to fit polymer syringes with exchangeable nozzles (Nordson Corporation, USA). A two-zone heating system is used to independently control the temperature in both sections of the printhead. First – the syringe heater –controlling the temperature of the polymer inside the syringe and second– the nozzle heater– controlling temperature of the polymer right at the nozzle.

Linear stages

A system of three linear actuators (OpenBuilds, USA) was used to control the print bed position along the x- and y-axis as well as printhead position along the z-axis. Similarly, aluminium extrusion-based solution provides the flexibility of the design while ensuring robustness and stability during the operation. A three-axis system of linear actuators comes with detailed assembly instructions. While the design provides a cost-effective solution that is suitable for most applications, the motion control system can be easily upgraded for more advanced applications.

Print bed

The print bed is a conductive and usually metallic surface that enables the collection of the printed fibres. Here, we used a $120 \times 120 \times 6$ mm aluminium block that provides sufficient printing area for most applications. The collector was assembled onto a gantry cart designed to run on an aluminium extrusion C-beam (OpenBuilds, USA).

Electrical assembly platform

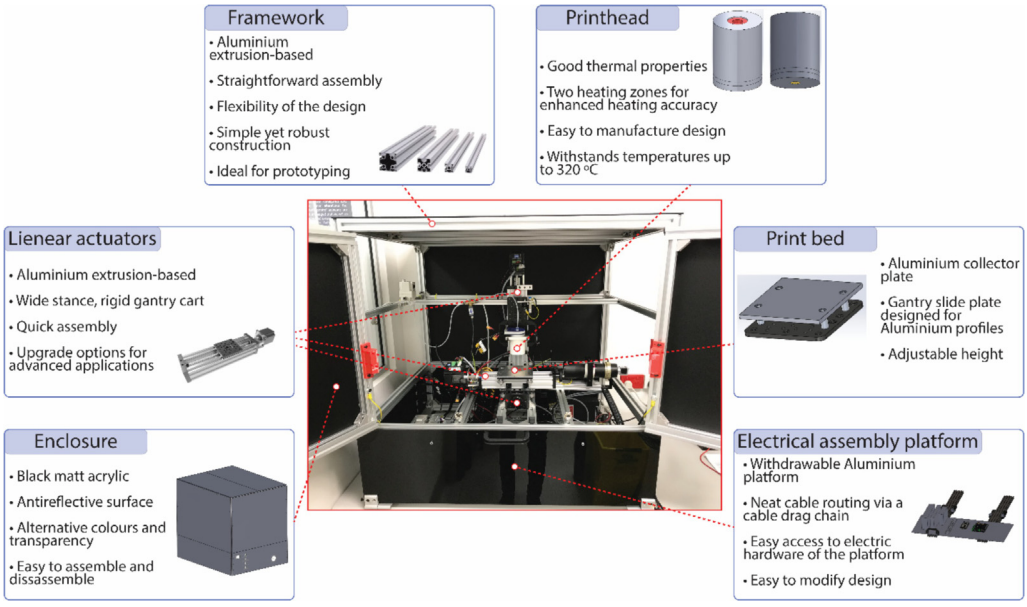

Fig. 2. Mechanical design overview of an Automated MEW platform. The platform consists of 3-axis linear actuator, aluminium extrusion-based framework, teflon printhead, aluminium print bed and withdrawable electrical assembly platform.

The electrical assembly platform is a 790 × 290 × 3 aluminium plate supported on two gantry carts where the electrical components are assembled. The withdrawable platform provides access to the electrical components to allow for troubleshooting and system modification.

3. Design files

See Table 2.
Mechanical build instructions – build instructions for the mechanical section of the build.

1) Electrical build instructions – build instructions for the electrical section of the build.
2) Software and firmware instructions – deployment instructions of the firmware and software.
3) Bill of materials – a spreadsheet including the components used for the build.
4) Design files (CAD) – CAD assembly of the platform.
5) PCB design files – schematic and layout of the PCB Arduino shield used in the platform.
6) Laser-cut parts (CAD) – a list of parts that required laser cutting.
7) Power distribution diagram – a power distribution circuit diagram of the platform.
8) Smoothieboard simplified connection diagram – a simplified circuit schematic of Smoothieboard connection diagram.
9) Arduino simplified connection diagram – a simplified version of Arduino connection diagram.
10) Python user interface – a Python user interface used to communicate with both microcontroller boards.
11) Arduino code – the Arduino firmware that was uploaded onto Arduino Due.

4. Bill of Materials

Bill of Materials is available in supporting documents in the Excel spreadsheet file "BOM_automated_MEW_platform.xlsx".

Table 2
Design file summary.

Design file name	File type	Open-source license	Location of the file
1) Mechanical instructions	PDF	CC BY-SA 4.0	Available with the article, Zenodo: https://doi.org/10.5281/zenodo.4699811
2) Electrical instructions	PDF	CC BY-SA 4.0	Available with the article, Zenodo: https://doi.org/10.5281/zenodo.4699811
3) Firmware and software instructions	PDF	CC BY-SA 4.0	Available with the article, Zenodo: https://doi.org/10.5281/zenodo.4699811
4) Bill of Materials (BOM)	XLSX	CC BY-SA 4.0	Available with the article, Zenodo: https://doi.org/10.5281/zenodo.4699811
5) Design files (CAD)	SLDPRT, SLDASM	CC BY-SA 4.0	Available with the article, Zenodo: https://doi.org/10.5281/zenodo.4699811
6) PCB design (Circuit diagram, PCB layout)	SchDot, pcbdoc	CC BY-SA 4.0	Available with the article, Zenodo: https://doi.org/10.5281/zenodo.4699811
7) Laser cut parts	SLDPRT, SLDASM	CC BY-SA 4.0	Available with the article, Zenodo: https://doi.org/10.5281/zenodo.4699811
8) Power distribution diagram	PDF	CC BY-SA 4.0	Available with the article, Zenodo: https://doi.org/10.5281/zenodo.4699811
9) Smoothieboard simplified connection diagram	PDF	CC BY-SA 4.0	Available with the article, Zenodo: https://doi.org/10.5281/zenodo.4699811
10) Arduino simplified connection diagram	PDF	CC BY-SA 4.0	Available with the article, Zenodo: https://doi.org/10.5281/zenodo.4699811
11) Python user interface	py	CC BY-SA 4.0	Available with the article, Zenodo: https://doi.org/10.5281/zenodo.4699811 GitHub: https://github.com/Lasonic/automated_mew_platform
12) Arduino code	ino	CC BY-SA 4.0	Available with the article, Zenodo: https://doi.org/10.5281/zenodo.4699811 GitHub: https://github.com/Lasonic/automated_mew_platform

5. Build instructions

Build instructions were divided into three parts: (1) mechanical assembly (linear stages, printhead, print bed framework), (2) electrical assembly (aluminium platform, cable carrier, Smoothieboard, Arduino, din terminals, power, safety and monitoring) and (3) software implementation (Arduino and Smoothieboard firmware, user interface). The description includes comments about possible design variations. Detailed step-by-step instructions for each section are uploaded as a supplementary document available in the GitHub repository. Suggested timeframes are given assuming basic skill level of mechanical, electrical and software engineering.

5.1. Mechanical implementation

Timing: 10.5 h
Materials: As listed in detailed instruction for each section.
Equipment: As listed in detailed instruction for each section.
Critical: As listed in detailed instructions for each section.

Linear actuators

Linear stages were designed and assembled in accordance with the OpenBuilds guidelines. OpenBuilds is an online platform that provides resources to open-source projects. The linear stages were built by following well-documented instructions and using suggested hardware. The design can be easily modified according to the requirements. For instance, the length of the linear stages can be adjusted by using different size of aluminium profiles. Similarly, the accuracy of the stages can be improved by upgrading the suggested in the design hardware.

Print bed

The Print bed consists of the aluminium collector and gantry cart, both being a part of the linear actuator system. The collector was mounted onto the gantry cart using countersink screws. Aluminium spacers were used to adjust the height of the collector plate. The collector height was designed around the location of the vision system and its proximity to the printhead. The gantry cart has several screw holes which open up the possibility to use collector plates of different geometries.

Printhead

The body of the cylindrical printhead is made of teflon. The syringe heater was fitted into the hollow cavity, while the nozzle heater was fitted into the bottom part of the printhead, which was connected with an additional teflon part via eight nylon screws. The additional teflon part contains a brass plate that is connected to the HV unit. The brass plate is the component that transfers the high electric potential to the nozzle.

Framework

The majority of the presented framework consists of 30 $\times$ 30 mm profiles that provide structural support, whereas 20 $\times$ 20 mm profiles were used for hardware mounting purposes. The profiles were connected using corner brackets providing flexibility of the solution while maintaining the robustness and structural stability. The framework design was dictated by the requirements of the monitoring hardware, such as the working distance of the lens, which can be adjusted to the desired specifications.

Enclosure

The final step of the platform assembly is the enclosure installation. A set of laser-cut 3.5 mm matt black acrylic panels were mounted using screws, hammer nuts and aluminium V-slot framework. The panels were attached on the outer side of the framework; therefore, the enclosure can be assembled anytime during the build. Flexible enclosure design allows for other material to be used instead of the acrylic panels.

5.2. Electrical implementation

Timing: 8.5 h
Materials: As listed in detailed instructions.
Equipment: As listed in detailed instructions.
Critical: As listed in detailed instructions.

Electrical assembly platform installation

The electrical assembly platform was constructed as a part of the framework. A 770 $\times$ 290 $\times$ 3 mm aluminium sheet mounted on two gantry carts and two 20 $\times$ 80 profiles was used as a base to assemble the electrical components of the MEW platform. The PSUs were grouped and placed next to the din terminals where the power is distributed. The electronic components were placed on the opposite side of the platform. Five cable carriers were installed across the platform to provide sufficient cable routing options. The components were mounted using screw holes. The assembly platform provides an easy way to access and, if required, modify the electrical design.

Cable carrier

Cable carriers were installed to provide a neat and convenient way of guiding electrical connections to sensors and actuators. Since the electrical components were mounted on the withdrawable aluminium platform, the cable carriers provide a great solution to maintain a secure and safe connection.

Smoothieboard

The Smoothieboard was connected to components that control the temperature and motion systems of the platform. Low-current connections were made using colour coded single and multi-core cables, while power connections were made using appropriately sized cables and Phoenix connectors. The Smoothieboard was wired as described in the attached instructions.

Arduino Due

Arduino Due was connected to the electronic devices using colour coded cables and custom designed Arduino PCB shield. The Arduino Due and PCB shield were constructed as presented in the attached instructions.

Din terminals

Din terminal blocks were mounted on the din aluminium rail attached to the electrical assembly plate. The din terminals distribute the power from the PSUs to the electrical devices. The screw-based din terminals provide a solderless and secure way of making electrical connections allowing for easy to implement design adjustments.

Safety

Non-contact magnetic switches are used with electromechanical relays to ensure safe access to the printer by a user. The switches were mounted between the frame and the main door of the platform. The HV unit is switched on when both of the front doors are closed. As soon as either of the door is open, the HV unit is disabled by disconnecting the power supply only to this unit.

Monitoring

A camera and lens were mounted together via C-Mount and connected to the computing unit via a USB3 cable. The camera and lens setup was designed to provide a very good image resolution while maintaining a large field of view in order to capture the process of fibre deposition. In the presented platform, the monitoring system design was the most important part of the design.

Illumination

An LED panel mounted in line with the camera axis was used to create a backlight illumination setup. For testing purposes, the LED panel is powered via an external PSU that allows for manual light intensity adjustment. Alternatively, the Smoothieboard provides a controllable 12VDC power output which can be used to power the LED panel.

5.3. Firmware and software implementation

Timing: 3 h
Materials: PC, connected Arduino Due and Smoothieboard with SD card.
Equipment: Internet connection.
Critical: Make sure the drivers are up to date.

Detailed step-by-step instructions of software and firmware implementation are attached in the supporting material. The computing unit is where the operations are executed. Here, a Windows 10 PC was used to install the essential drivers and software. The instructions include the resources required to properly establish the firmware and software of the MEW platform.

6. Operation instructions

This section describes how to use the MEW platform and avoid any potential safety hazards. All build instruction steps should be completed in order to ensure the smooth and safe operation of the platform.

Axes home position

Firstly, set the home position for all three axes to the location shown in Supporting Fig. S1A. This can be done by positioning the axes manually before turning on the platform. A home position can also be specified using 'G28.3′ G-code. It is important to set the home position since the current version of the platform does not include the limit switches. The physical limits of the axes can be manually set in the configuration file of the Smoothieboard.

Platform initialisation

1) Make sure at least one of the printer's doors is opened to make sure the HV unit is turned off.
2) Connect the mains power to the printer using an IEC cable.
3) Connect the pressure regulator to the air (or other suitable gas) pressure source.
4) Connect the camera to the USB3 port of the processing PC.
5) Turn on the power using the mains switch. All motors should have their green LED illuminated (see Supporting Fig. S1B).
6) Turn the computing PC on. "ON" LED on Arduino and "VBB" LED on Smoothieboard should be illuminated (see Supporting Fig. S1C, D).

Default system settings are already uploaded onto the Arduino board:

- Pressure – 0 kPa
- High Voltage – 0 kV
- Syringe setpoint temperature – Not set
- Nozzle setpoint temperature – Not set
- Collection speed – 4000 mm/min
- Working distance – 0 mm

7) Copy a G-code file to be executed onto the SD card of the Smoothieboard.
8) Open previously installed "Pylon Viewer", select the connected camera and start live preview. For detailed instructions refer to the setup guide "Pylon_Viewer_Instalation_and_Setup_Guide.pdf" available in supporting materials.

Serial communication protocol and commands

Serial communication is established with both Smoothieboard and Arduino Due. While Smoothie offers a wide range of well-documented G-code and console commands for communication purposes, a custom communication protocol was developed to communicate with Arduino. Details regarding a communication format with Arduino can be found in Supporting Fig. S2 while the most useful Smoothie commands are listed in Supporting Table T2.

1) Start serial communication with Smoothieboard and Arduino via Python user interface by executing the Python file "automated_mew_platform_user_interface.py".

Important note: If Smoothieboard and Arduino were connected correctly, the program should print "Connected to Smoothieboard!" and "Connected to Due!". If the connection cannot be established with either of the boards, check electrical and software instructions of Arduino and Smoothieboard to make sure the wiring and software initialisation was performed correctly.

2) Select the board to receive the command and press "Enter".
3) Type in the command and press "Enter".
4) A message will be printed if the command was successfully transmitted or not. A return message will be displayed if applicable for a given command.
5) The command is executed in the background while the program starts again from step 2).

Important note: If you notice problems with serial communication, try resetting the program. Alternatively, for Spyder users try the following:

- When the program does not respond, press "Ctrl + ." to reset the kernel.
- When the program is stuck reading or sending a serial packet press "Ctrl + c" to interrupt.

Input parameter selection

1) Select input parameters. Supporting Fig. S3 shows an example of the parameter selection process using Python user interface in Spyder.
2) Close printer's main doors to enable HV connection.

WARNING In case of arcing, it is highly recommended to cut off the power supply to the HV unit either by opening the main door of the platform or switching off the mains power supply to the platform. Although the platform is well-protected by appropriate earthing and the HV unit having overload, short circuit and reverse polarity protection, there is always a risk of damaging electronic components that are vulnerable to an electric discharge.

3) Once input parameters are set, wait a few minutes for the temperature of the material to reach the desired level.
4) Observe live video recording focused on the area between the nozzle and print bed.
5) Send 'play /sd/file_name.txt' command to Smoothieboard to start the printing process. This will execute the G-code file named 'file_name.txt' stored on the SD card.

7. Validation and characterization

This section presents a case use of the MEW automated platform. The successful design, assembly and operation of the platform were demonstrated with a series of short experiments.

7.1. Melt electrowritten scaffolds

The presented MEW platform was used to 3D print scaffolds architectures that are often used in the Regenerative Medicine and Tissue Engineering field. A 20 × 100 mm 10-layer scaffold was printed to demonstrate the ability of the platform to accurately fabricate polymer structures. Fig. 3 shows images of the printed structure displaying well-organised and perfectly

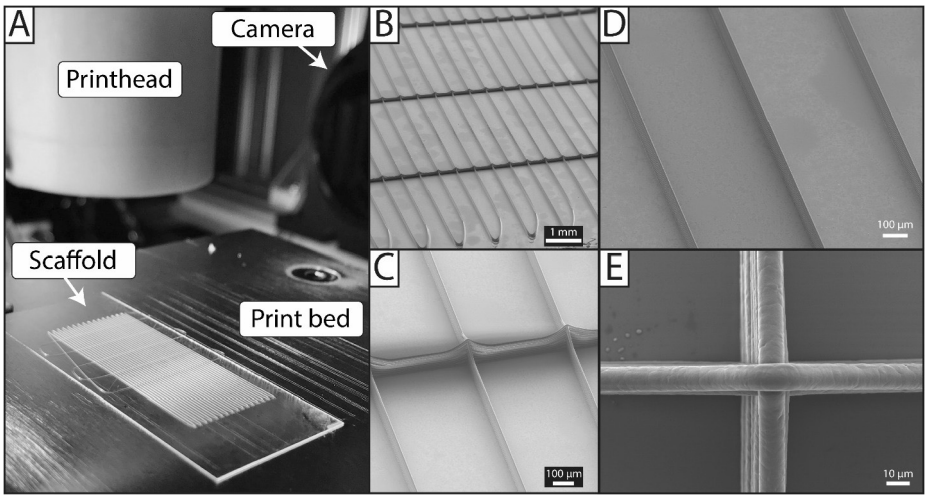

Fig. 3. (A) Example of a scaffold printed over a glass slide on a flat collector using MEW platform. (B–E) SEM images show precisely printed and accurately stacked medical grade polycaprolactone fibres.

stacked fibres. Supporting video S1 demonstrates the printing process from the user perspective while Supporting video S2 showcases in detail the process of fibre deposition.

7.2. Input process parameters evaluation

Each process parameter was evaluated to demonstrate the platform's performance. Parameters can be changed in real-time during the operation via the Python user interface or automatically using other custom-developed programs (e.g. Matlab).

7.2.1. Temperature

Temperature control was evaluated by assessing the time response of the heating system. The starting temperature of the nozzle and syringe heaters were 32 °C and 42 °C, respectively. The setpoint temperature was defined at 85 °C. Fig. 4 shows the recorded temperature reading. While the temperature of the nozzle heater rises slower than the syringe heater, it does

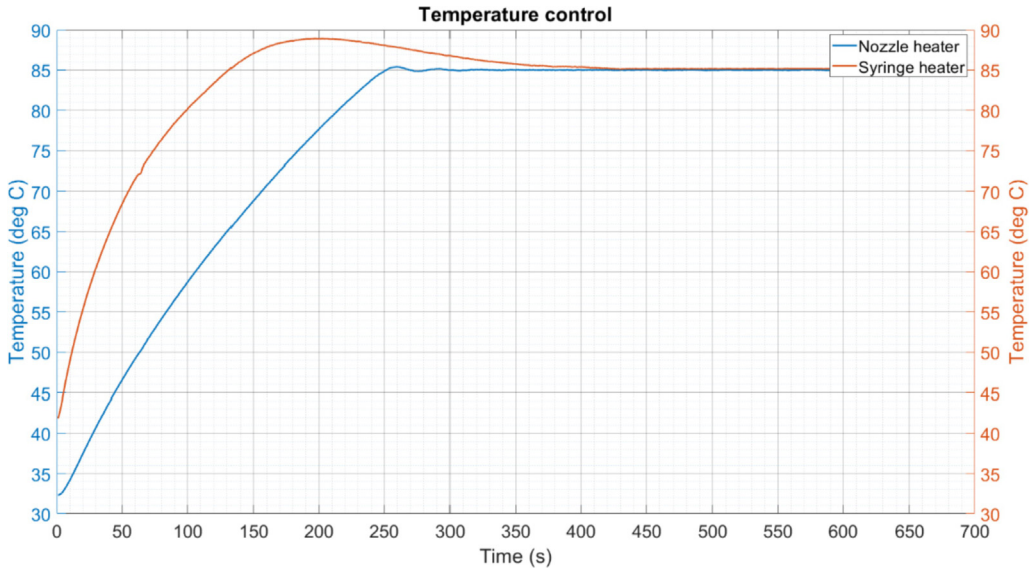

Fig. 4. Temperature control time response. The syringe heater increases the temperature faster, however, it overshoots more and takes longer to reach the steady state. Although the nozzle heater takes longer to reach the setpoint, the overshoot is minimal and the steady state is achieved earlier. Both heaters demonstrate a very good ability to maintain the desired temperature.

not overshoot as significantly as the syringe heater. Both heaters show a very good response with a minimal steady state error of < 1 °C.

7.2.2. Pressure

The study and analysis of the pressure control was performed by setting the pressure at different levels to test the reliability and accuracy of the control and monitoring system. The initial output pressure was set to 100kPa and was reduced numerous times by 5 kPa. Fig. 5 shows the recorded output pressure. This demonstrates that the system successfully executed each command. Although output reading noise was present, the mean value of each pressure change confirms the desired pressure value.

7.2.3. High voltage

The performance of the HV unit was evaluated by gradually increasing the output voltage from 0 to 5 kV. Fig. 6 shows the data recorded by the HV output monitor. The results show the voltage being successfully increased to the desired level. The recorded voltage spikes were attributed to the noisy HV output monitoring signal as the quality of the previously presented scaffold proves the steady HV output.

7.2.4. Collection speed and working distance - linear actuators

The accuracy of both collection speed and working distance are dependent on the performance of linear actuators. Although the step loss is minimised by the closed-loop operation of the stepper motors, the positioning accuracy can be affected while using high microstepping that sacrifices the positioning accuracy for resolution. In the presented MEW platform, the z-axis carries the most load. Therefore, the accuracy of that axis was evaluated by displacing the printhead between two predefined positions [26]. The position after each translation was recorded using the high-resolution camera and measured using image analysis tools. A set for each position consists of 50 data points. Fig. 7 shows the positioning error of the z-axis linear actuator for each position. The mean positioning error of position 1 and 2 is 15 and 16 μm, respectively.

7.3. Monitoring system evaluation

The capability of the monitoring system was demonstrated by analysing process signatures of the system during printing using Matlab. The algorithm itself was not the focus of this study and was used as an evaluation tool. The live footage from the process was analysed in real-time by measuring Taylor cone area, jet angle and fibre diameter as shown in Fig. 8.

Two different configurations of input parameters were used to demonstrate the ability of the platform to detect different printing conditions through monitoring and analysis of the system output. The applied pressure was the only adjusted parameter, while other parameters were kept constant. Table 3 shows the parameter configuration used for the experiment. The system was able to accurately detect two different responses of the system across all three process signatures.

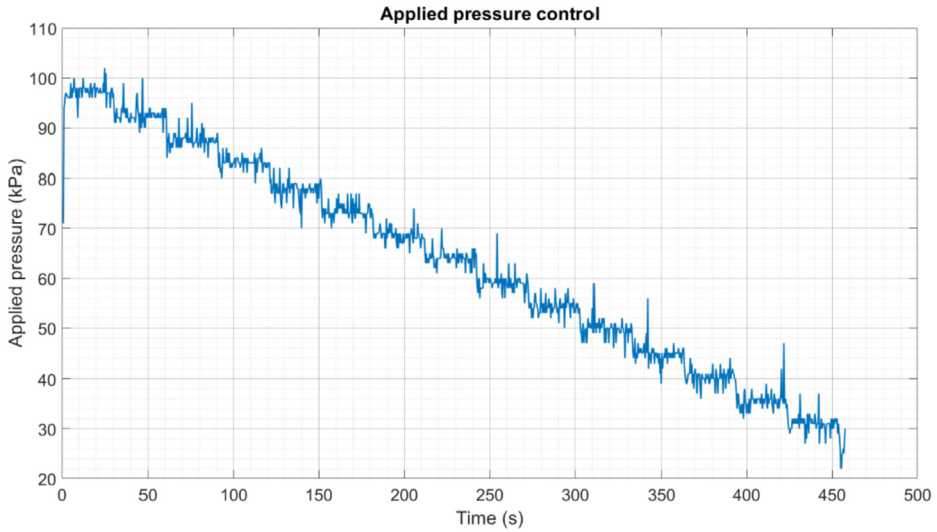

Fig. 5. Applied pressure control. The graph shows that pressure can be accurately and automatically set to the desired value. In this case, the pressure was decreased by 5 kPa every 30 s.

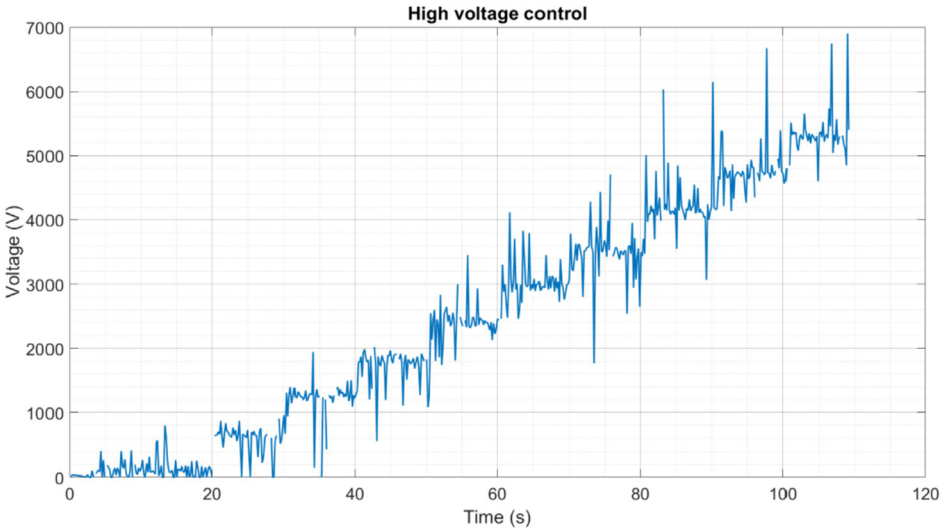

Fig. 6. High voltage control. The graph demonstrates real-time high voltage control and monitoring. High voltage was gradually increased while the recorded voltage output was recorded. The noise present in the reading is attributed to the reading noise as the printed structures suggest the steady HV output.

7.3.1. Taylor cone area

In MEW, the Taylor cone is a small volume of polymer created at the tip of a nozzle when pressure is applied to the molten polymer stored in the syringe. When HV is applied, it often takes a several minutes until a micro-sized jet is ejected towards the collector plate. The Taylor cone size reveals important characteristics of the process such as stability of the process. Although the Taylor cone size represents a volume of the polymer, the Taylor cone area can be obtained from a 2D image and is a very good estimation of its size. Fig. 9 demonstrates the behaviour of the Taylor cone area at two different parameter configurations. The results indicate less material oscillation at the pressure of 100 kPa and more material oscillation at 200 kPa.

7.3.2. Jet angle

The jet angle is defined as the angle between the centre of the nozzle tip and the deposition point of the polymer onto the collector. The Jet angle is an important process signature that provides information about the stability and shape of the fibre

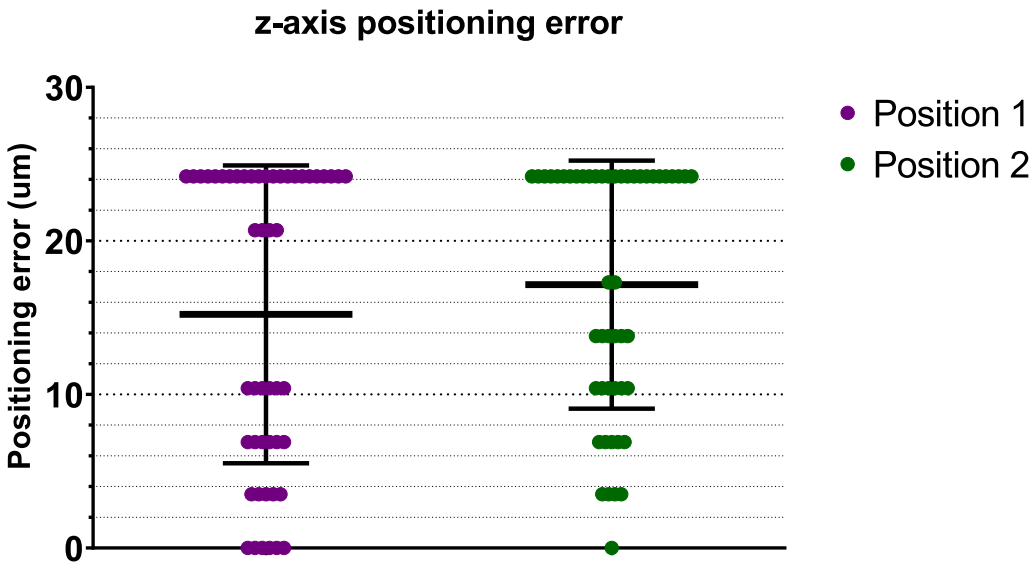

Fig. 7. Z-axis positioning validation. The results show a small mean error of 15 μm for Position 1 and 17 μm for Position 2.

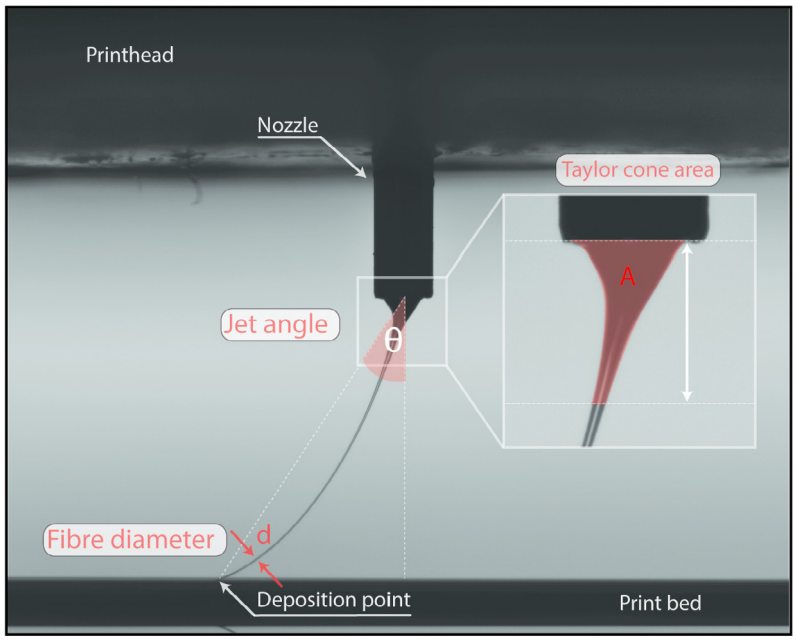

Fig. 8. Diagram demonstrating MEW output parameters analysis. The high-resolution camera and image analysis algorithm are used to measure the Taylor Cone area, jet angle and fibre diameter in real-time.

Table 3
Parameter configurations used for the validation experiment. High voltage, syringe temperature, nozzle temperature, working distance and collection speed were kept constant across both configurations at 5 kV, 85 °C, 85 °C, 3.8 mm, 800 mm/min, respectively, while applied pressure was changed from 100 kPa to 200 kPa.

	Parameter configuration 1	Parameter configuration 2
Applied pressure	100 kPa	200 kPa
High voltage	5 kV	5 kV
Syringe temperature	85 °C	85 °C
Nozzle temperature	85 °C	85 °C
Working distance	3.8 mm	3.8 mm
Collection speed	800 mm/min	800 mm/min

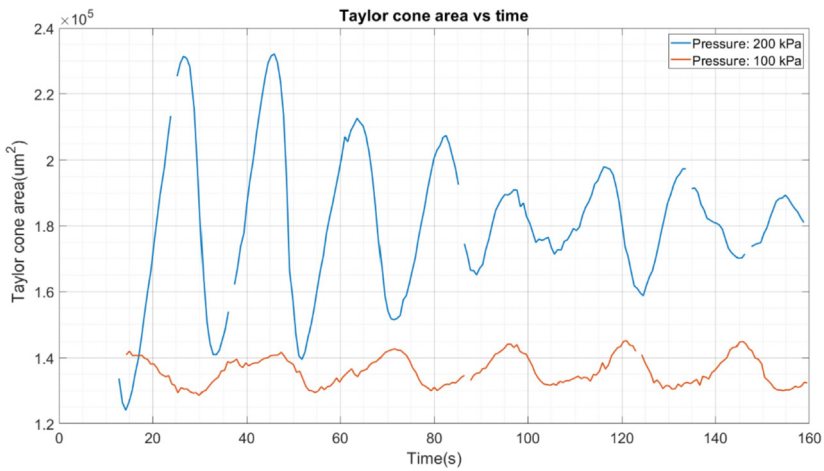

Fig. 9. Taylor cone area monitoring results. The system can clearly detect changes occurring when input parameters are changed. Here, two different pressure levels show very different behaviour of the Taylor cone area.

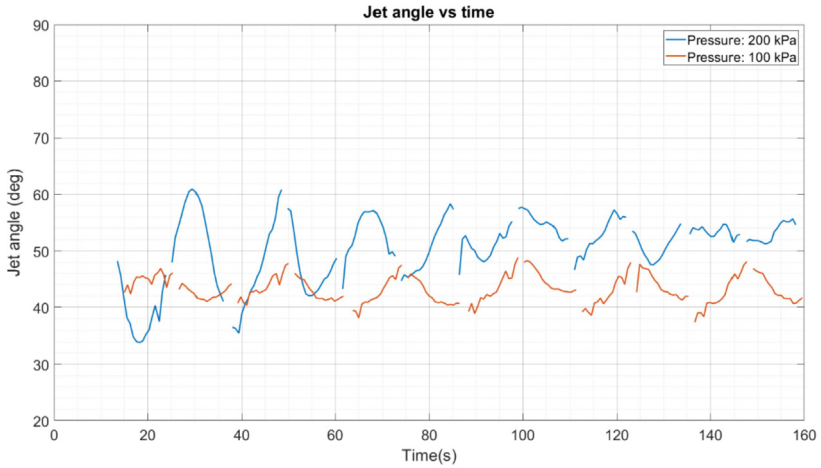

Fig. 10. Jet angle monitoring results demonstrate larger and smaller amplitude of oscillations at 200 kPa and 100 kPa, respectively.

deposition. Fig. 10 demonstrates the recorded behaviour of the jet angle. The results show jet angle oscillations in both cases with larger amplitude oscillation generated by 200 kPa pressure.

7.3.3. Fibre diameter

The fibre diameter refers to the diameter of the fibre deposited onto a collector. It defines the quality of the printed structures and acts as a reproducibility measure of the process. Fibre diameter variation is usually an unwanted phenomenon caused by the instability of the printing process. The instability often occurs when the input parameters are incorrectly selected. Fig. 11 shows that the pressure of 200 kPa caused a large fibre diameter oscillation. Although at the pressure level of 100 kPa the oscillation still occurred, the diameter variation is significantly smaller. This indicates better stability and reproducibility of the process at the pressure of 100 kPa.

7.4. Advanced operation

Finally, the presented MEW platform was used to perform a more advanced experiment where the applied pressure input was defined as a sine wave with 170 kPa offset, 40 kPa amplitude and 20 s period. Fig. 12 shows the response of the Taylor cone area to a time-varying pressure input. The results demonstrate the capability of the platform to perform analysis of

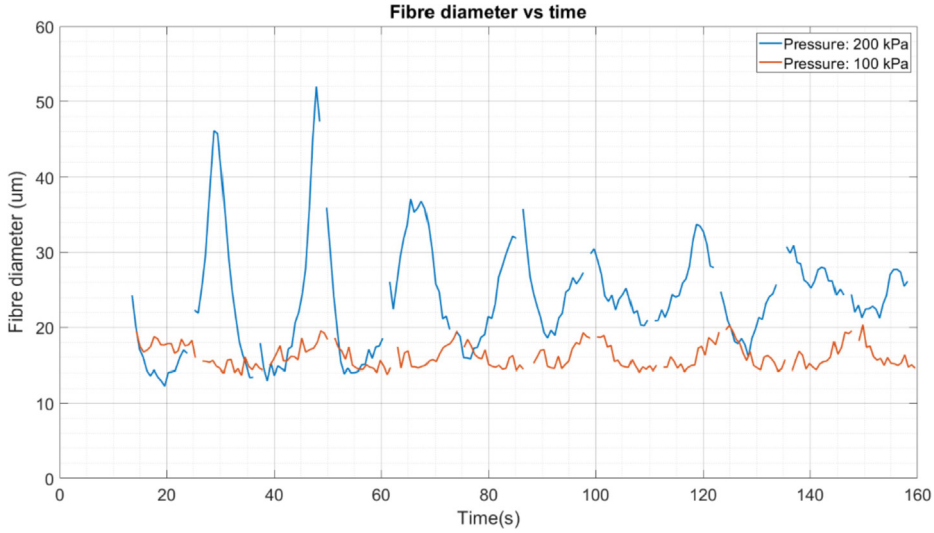

Fig. 11. Fibre diameter monitoring results. Fibre diameter experiences a significantly higher amplitude oscillation at 200 kPa while showing notably less diameter variation at 100 kPa.

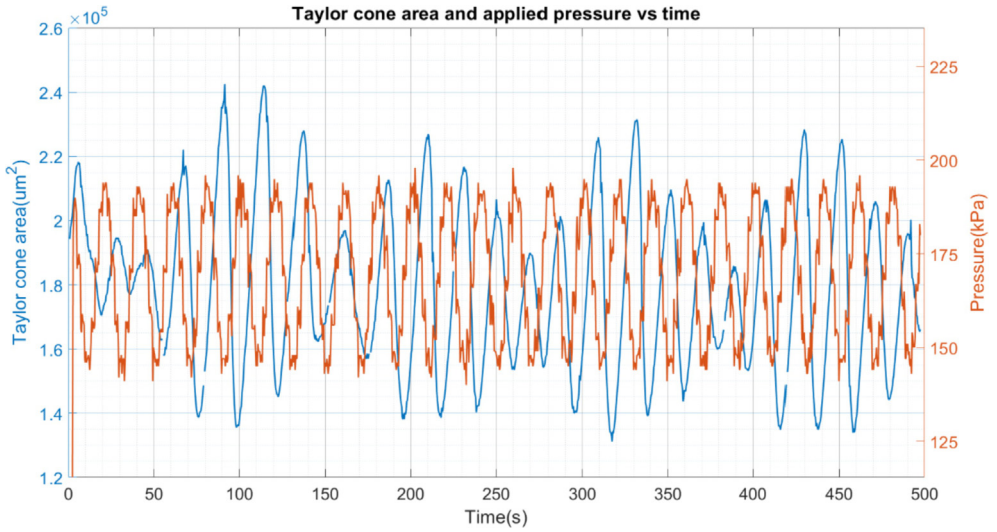

Fig. 12. Taylor cone area output subject to a periodic input of the applied pressure. The oscillating input creates a complex oscillatory response of the Taylor cone area. The results demonstrate the capability of the platform to perform complex experiments which can be used to establish more accurate models of the MEW process.

complex, time-varying input parameter configurations, which can be further used to establish more accurate models of the MEW printing process.

8. Conclusion and future work

In summary, most of the currently available MEW hardware is still designed and manufactured in academic lab settings or as poorly performing add-on device of bioprinters. Henceforth, creates issues with replication of the results across different MEW devices. Additionally, the lack of real-time parameter monitoring and control further hinders the technological advancement of the technique. Here, we address these issues with a low-cost and open-source automated MEW platform with real-time process parameter monitoring and control functionality. The presented setup provides users with the ability to monitor and control the printing process while collecting the data that can be used for further analysis. The design of the platform is flexible and additional improvements can be readily implemented according to the specific needs. In the future, we hope that the open-source nature of the presented platform will improve the accessibility of MEW and help to drive the technological development of the technique.

Declaration of Competing Interest

The authors declare that they have no known competing financial interests or personal relationships that could have appeared to influence the work reported in this paper.

Acknowledgements

This work was supported by the Australian Research Council (ARC) Industrial Transformation Training Centre in Additive Biomanufacturing [IC 160100026] and by the ARC Industrial Transformation Training Centre for Multiscale 3D Imaging, Modelling, and Manufacturing [IC 180100008] and Centre in Transformative Biomimetics in Bioengineering, Queensland University of Technology. P.M. was supported by QUT's Postgraduate Research Award.

The authors acknowledge the members of the Centre in Regenerative Medicine at QUT, in particular Aaron Foster and Peter Bate for their technical support. Daniel Mapson for electrical engineering support and certification, Harry Basil and Marwan Suheimat for optical design support, Fanny Blaudez for proofreading. We would like to thank P. Dalton for valuable discussion of the state of the art of technology and proofreading of the manuscript.

Human and animal rights

The work did not involve the use of any human or animal subjects.

Appendix A. Supplementary data

Supplementary data to this article can be found online at https://doi.org/10.1016/j.ohx.2021.e00246.

References

[1] F.P.W. Melchels, J. Feijen, D.W. Grijpma, A review on stereolithography and its applications in biomedical engineering, Biomaterials 31 (2010) 6121–6130.
[2] P.S. D'Urso, D.J. Effeney, W.J. Earwaker, T.M. Barker, M.J. Redmond, R.G. Thompson, F.H. Tomlinson, Custom cranioplasty using stereolithography and acrylic, Br. J. Plast. Surg. 53 (3) (2000) 200–204.
[3] G. Wurm, B. Tomancok, K. Holl, J. Trenkler, Prospective study on cranioplasty with individual carbon fiber reinforced polymere (CFRP) implants produced by means of stereolithography, Surg. Neurol. 62 (6) (2004) 510–521.
[4] S. Singh, S. Ramakrishna, Biomedical applications of additive manufacturing: present and future, Curr. Opin. Biomed. Eng. 2 (2017) 105–115.
[5] L.E. Murr, S.M. Gaytan, F. Medina, H. Lopez, E. Martinez, B.I. Machado, et al, Next-generation biomedical implants using additive manufacturing of complex, cellular and functional mesh arrays, Philos. Trans. R. Soc. A 368 (2010) 1999–2032.
[6] G.J. Schiller, Additive manufacturing for aerospace, in: 2015 IEEE Aerospace Conference, 2015, pp. 1–8.
[7] P.A. Kobryn, N.R. Ontko, P.L. Perkins, J.S. Tiley, Additive manufacturing of aerospace alloys for aircraft structures, AVT-139 Specialists' Meeting in Amsterdam 139 (2006) 1–14.
[8] R. Liu, Z. Wang, T. Sparks, F. Liou, J. Newkirk, 13 – Aerospace applications of laser additive manufacturing, in: Laser Additive Manufacturing, Elsevier, 2017, pp. 351–371, https://doi.org/10.1016/B978-0-08-100433-3.00013-0.
[9] L. Jyothish Kumar, C.G. Krishnadas Nair, Current trends of additive manufacturing in the aerospace industry, in: David Ian Wimpenny, Pulak M. Pandey, L. Jyothish Kumar (Eds.), Advances in 3D Printing & Additive Manufacturing Technologies, Springer Singapore, Singapore, 2017, pp. 39–54, https://doi.org/10.1007/978-981-10-0812-2_4.
[10] André Luiz Jardini, Maria Aparecida Larosa, Cecília Amélia de Carvalho Zavaglia, Luis Fernando Bernardes, Carlos Salles Lambert, Paulo Kharmandayan, Davi Calderoni, Rubens Maciel Filho, Customised titanium implant fabricated in additive manufacturing for craniomaxillofacial surgery, Virtual Phys. Prototyping 9 (2) (2014) 115–125.
[11] Yu-an Jin, Jeff Plott, Roland Chen, Jeffrey Wensman, Albert Shih, Additive Manufacturing of Custom Orthoses and Prostheses – A Review, Proc. CIRP 36 (2015) 199–204.
[12] Mika Salmi, Kaija-Stiina Paloheimo, Jukka Tuomi, Jan Wolff, Antti Mäkitie, Accuracy of medical models made by additive manufacturing (rapid manufacturing), J. Cranio-Maxillofac. Surg. 41 (7) (2013) 603–609.
[13] M. Castilho, A. van Mil, M. Maher, C.H.G. Metz, G. Hochleitner, J. Groll, et al, Melt Electrowriting Allows Tailored Microstructural and Mechanical Design of Scaffolds to Advance Functional Human Myocardial Tissue Formation, Adv. Funct. Mater. 28 (2018/10/01 2018.) 1803151.
[14] Hajun Lee, Yeonwoo Jang, Jun Kyu Choe, Suwoo Lee, Hyeonseo Song, Jin Pyo Lee, Nasreena Lone, Jiyun Kim, 3D-printed programmable tensegrity for soft robotics, Sci. Robot. 5 (45) (2020), https://doi.org/10.1126/scirobotics.aay9024.
[15] F.J. O'Brien, Biomaterials & scaffolds for tissue engineering, Mater. Today 14 (2011) 88–95.
[16] S.V. Madihally, H.W.T. Matthew, Porous chitosan scaffolds for tissue engineering, Biomaterials 20 (1999) 1133–1142.
[17] D.W. Hutmacher, Scaffolds in tissue engineering bone and cartilage, Biomaterials 21 (2000) 2529–2543.
[18] T.D. Brown, P.D. Dalton, D.W. Hutmacher, Direct writing by way of melt electrospinning, Adv. Mater. 23 (2011) 5651–5657.
[19] Toby D. Brown, Fredrik Edin, Nicola Detta, Anthony D. Skelton, Dietmar W. Hutmacher, Paul D. Dalton, Melt electrospinning of poly(ε-caprolactone) scaffolds: Phenomenological observations associated with collection and direct writing, Mater. Sci. Eng. C 45 (2014) 698–708.
[20] Paul D. Dalton, Melt electrowriting with additive manufacturing principles, Curr. Opin. Biomed. Eng. 2 (2017) 49–57.
[21] Thomas M. Robinson, Dietmar W. Hutmacher, Paul D. Dalton, The Next Frontier in Melt Electrospinning: Taming the Jet, Adv. Funct. Mater. 29 (44) (2019) 1904664, https://doi.org/10.1002/adfm.v29.4410.1002/adfm.201904664.
[22] Navid T. Saidy, Tara Shabab, Onur Bas, Diana M. Rojas-González, Matthias Menne, Tim Henry, Dietmar W. Hutmacher, Petra Mela, Elena M. De-Juan-Pardo, Melt Electrowriting of Complex 3D Anatomically Relevant Scaffolds, Front. Bioeng. Biotechnol. 8 (2020), https://doi.org/10.3389/fbioe.2020.00793.
[23] G. Hochleitner, A. Youssef, A. Hrynevich, J.N. Haigh, T. Jungst, J. Groll, et al, Fibre pulsing during melt electrospinning writing, BioNanoMaterials 17 (2016) 159–171.
[24] Felix M Wunner, Pawel Mieszczanek, Onur Bas, Sebastian Eggert, Joachim Maartens, Paul D Dalton, Elena M De-Juan-Pardo, Dietmar W Hutmacher, Printomics: the high-throughput analysis of printing parameters applied to melt electrowriting, Biofabrication 11 (2) (2019) 025004, https://doi.org/10.1088/1758-5090/aafc41.
[25] F.A. Alexander, L. Johnson, K. Williams, K. Packer, A Parameter Study for 3D-Printing Organized Nanofibrous Collagen Scaffolds Using Direct-Write Electrospinning, Materials vol. 12, 2019.
[26] Sebastian Eggert, Pawel Mieszczanek, Christoph Meinert, Dietmar W Hutmacher, OpenWorkstation: A modular open-source technology for automated in vitro workflows, HardwareX 8 (2020) e00152, https://doi.org/10.1016/j.ohx.2020.e00152.
[27] Pawel Mieszczanek, Thomas M Robinson, Paul D Dalton, Dietmar W Hutmacher, Convergence of Machine Vision and Melt Electrowriting, Advanced Materials 33 (29) (2021), https://doi.org/10.1002/adma.202100519.

Pawel Mieszczanek is a PhD student in engineering at Queensland University of Technology, Australia. His interest in translation of digital technology in biomedical industry led him to Gelomics where he worked as a mechatronics engineer. He committed to innovation accelerator programs focusing on digitalization of additive manufacturing. His research interests include advanced manufacturing technology and its applications.

Sebastian's research passion lies in interdisciplinary projects taking place at the borders where engineering and physics meet biology and medicine. His studies at the Technical University of Munich (TUM, Germany) and his PhD at the Queensland University of Technology (QUT, Australia) provided him with a strong engineering background and in-depth knowledge of biological and chemical systems. As the Chief Scientific Officer (CSO) at cellasys GmbH (Germany), he is currently developing novel metabolic monitoring solutions for 3D cell culture models.

DProf Corke is a robotics researcher and educator. He is the distinguished professor of robotic vision at Queensland University of Technology, and director of the QUT Centre for Robotics. He created widely used open-source software for teaching and research, wrote the best selling textbook "Robotics, Vision, and Control", and created the Robot Academy open online learning resources. He is a fellow of the IEEE, the Australian Academy of Technology and Engineering, and the Australian Academy of Science, and sits on the advisory boards of a number of technology startups.

DProf Hutmacher is an engineer, a scholar, an educator, an inventor, an entrepreneur. He is committed to fostering transformative fundamental and applied research and pedagogical innovation as well as programs that create an entrepreneurial mindset amongst academicians and students. Prof Hutmacher is an internationally recognized leader in the fields of biomaterial science, bioengineering, computational modelling and advanced manufacturing.